AIAA 2017-4092
AIAA AVIATION Forum
5-9 June 2017, Denver, Colorado
17th AIAA Aviation Technology, Integration, and Operations Conference

Design Space Exploration for Hybrid Solar/Soaring Aircraft

John J. Bird* and Jack W. Langelaan†
The Pennsylvania State University, University Park, PA 16802 USA

While solar power is attractive as an aircraft energy source, its low power density compromises the maximum speed of solar aircraft. When flying within the lower troposphere, convective updrafts can be used to augment solar power. Soaring speed to fly theory is adapted to predict the performance of sailplanes equipped with solar arrays. This is used to determine the sensitivity of hybrid solar/soaring flight to aerodynamic performance, weight, and power use strategy. Solar augmentation offers the potential to substantially enhance sailplane performance.

I. Introduction

Aircraft that exploit both updrafts and solar energy date to the first piloted solar aircraft.[1] At the time, solar cells could not provide enough power for even motorized ultralight gliders such as Solar Riser and Sunseeker. These aircraft would soar while using solar power to charge a battery, allowing periodic motor runs. Solar cells and batteries have matured to the point that a number of large solar aircraft have been constructed, both autonomous and piloted.[2] While capable of extreme endurance, these aircraft are slow and fragile. They must operate only in favorable conditions or else must climb into the stratosphere to avoid turbulence.

These improved cells and batteries have also made low altitude persistent solar aircraft possible.[3–5] These aircraft share many characteristics with sailplanes – the use of uncertain, distributed energy, and small average power output (the equivalent power in a thermal climb can be considerable for sailplanes but is balanced by unpowered cruise). Solar and soaring aircraft occupy similar design envelopes, with low wing loading relative to conventional aircraft and high aerodynamic efficiency.

These similarities motivate the concept of hybrid solar-soaring aircraft. While several solar sailplanes such as Icare[6] and Sunseeker Duo[7] have been constructed and the solar UAS SoLong has used thermals,[2] the low wing loading required for pure solar flight limits their maximum speed and payload. The design space examined in this paper is distinct from existing solar aircraft and previous examinations of solar-powered competition sailplanes[6,8] in that we do not explicitly seek designs capable of sustained solar flight. Instead the objective is to maximize the performance of an aircraft which can exploit both solar energy and soaring, permitting flight with wing loading higher than pure solar flight allows and higher average speed than can be achieved solely by thermalling.

This paper adapts performance analysis methods from soaring, deriving expressions to predict the performance of solar/soaring hybrid aircraft. These relations are then used to explore the design space for these aircraft, with a focus on hybrids as a new class of racing sailplane. The results are also applicable to efficient, long-range UAS.

II. Solar Aircraft Performance

II.A. Soaring Aircraft

Soaring speed to fly theory was known in the 1930s, developed in tandem with thermal soaring.[9,10] It has since been extended to provide a framework for analyzing the performance of aircraft with intermittent energy inputs and guiding their operation.[11–15]

*PhD Candidate, Department of Aerospace Engineering, Student Member AIAA.
†Associate Professor, Department of Aerospace Engineering, Associate Fellow AIAA.

For completeness, we will briefly review speed to fly theory. Figure 1 illustrates the flight path used for the speed to fly calculation. The aircraft stops and climbs in updrafts then cruises between thermals at constant speed. The speed to fly is determined by the next updraft strength, the inter-thermal up or downdraft environment, and the sailplane's gliding performance. It is assumed that the spacing of thermals and depth of the boundary layer must be such that the next thermal can always be reached from the previous at the optimal speed.

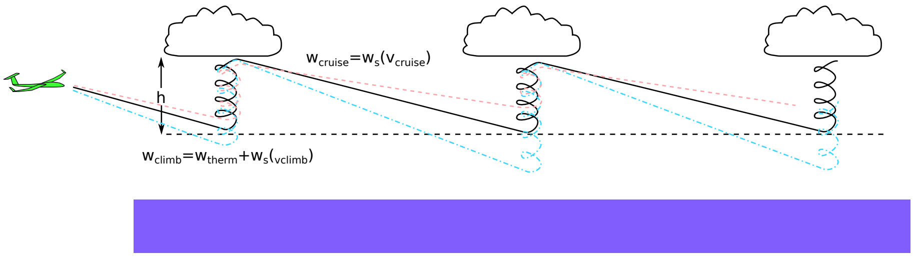

Figure 1: The speed to fly derivation assumes constant, known climb rates in thermals and constant inter-thermal cruise speeds. Thermals are assumed to be spaced closely enough that the next thermal can always be reached from the previous at the optimal speed. The paths of three gliders are illustrated here. The optimal in black, one which flies to slowly in red, and another which flies too fast in light blue. Flying slowly reduces the time spent climbing but less progress is made overall while flying too fast reduces average speed because of the increased time spent climbing.

Gliding performance of the aircraft is characterized by a "speed polar" which relates airspeed to vertical speed. This provides a useful analytic tool, expressing the power required to sustain flight as specific energy rate, which has units of speed allowing it to be related to instrument indications. The speed polar is frequently approximated as a second order polynomial:

$$w_s(V) = aV^2 + bV + c \tag{1}$$

The vertical speed, $w_s(V)$ is always negative, as it represents the descent rate required to maintain flight at constant speed, so it is often referred to as the sink rate. We follow Reichmann's convention[13] where sink rate is required to be negative ($w_s(V) < 0$) in all computations but the reader should be cautioned that the term is often used colloquially without a sign, the negative being implicit.

Because the aircraft performance is defined in specific power, we find it convenient to express the solar energy input in specific power as well, dividing the energy gathered by the solar panels by the aircraft weight:

$$p_{pv} = \frac{P_{pv}}{mg} = \frac{S_{panel} I \eta_{pv}}{mg} \tag{2}$$

Where S_{panel} represents the area of the solar array, I the solar insolation, and η_{pv} the efficiency of the conversion from solar to aerodynamic power (including solar cell, MPPT, motor, and propeller efficiency). This formulations allows p_{pv} to have a clear physical interpretation: the degree to which solar power can offset the aircraft sink rate, so that if $w_s(V) + p_{pv} > 0$ the aircraft is climbing. Expressed in this way, solar power is mathematically identical to a vertical updraft, making it straightforward to include in an analysis of soaring performance.

II.B. Hybrid Solar-Soaring

With reference to figure 1, we develop speed to fly with solar power, here assuming that the inter-thermal environment is quiescent. As in traditional speed to fly theory, inter-thermal cruise speed is constant at V_c, while during climbs the aircraft is circling and makes no progress toward the goal. A pure soaring climb rate is determined by the sum of updraft strength and sink rate $w_{climb} = w_{therm} + w_s(V_{climb})$ where w_s represents the speed dependent sink rate of the aircraft and w_{therm} the updraft velocity. Thermals are assumed uniform so that w_{climb} is constant. The effect of solar augmentation is then included with a specific power term $p_{pv} = \frac{P_{pv}}{mg}$ so that the total time to climb height, h is:

$$t_{climb} = \frac{h}{w_{climb} + p_{pv}} \tag{3}$$

Likewise the time spent in cruise descending from height h is determined by the sink rate, which varies with speed $w_s(V_{cruise})$ and the solar power input p_{pv}.

$$t_{cruise} = \frac{-h}{w_s(V_{cruise}) + p_{pv}} \tag{4}$$

The mean cross-country speed attained is then:

$$\overline{V} = \frac{\Delta X}{\Delta t} = \frac{V_{cruise}\ t_{cruise}}{t_{cruise} + t_{climb}} \tag{5}$$

Substituting equations 3 and 4 and simplifying, the cross-country speed can be expressed.

$$\overline{V} = -V_{cruise}\frac{w_{climb} + p_{pv}}{w_s(V_{cruise}) - w_{climb}} \tag{6}$$

To find the optimal cruise speed, a derivative with respect to V_{cruise} is taken and the resulting expression set equal to zero.

$$\begin{aligned}\frac{\partial \overline{V}}{\partial V_{cruise}} = 0 = \\ \frac{(w_{climb} + p_{pv})(w_{climb} - w_s(V_{cruise})) - \frac{\partial w_s(V_{cruise})}{\partial V_{cruise}}(w_{climb} + p_{pv})V_{cruise}}{(w_{climb} - w_s(V_{cruise}))^2}\end{aligned} \tag{7}$$

Removing any expression common to the two terms in the numerator:

$$\frac{\partial \overline{V}}{\partial V_{cruise}} = 0 = w_{climb} - w_s(V_{cruise}) + \frac{\partial w_s(V_{cruise})}{\partial V_{cruise}}V_{cruise} \tag{8}$$

Immediately a surprising observation can be made – the optimal speed is independent of solar power input. This has obvious advantages with respect to control strategy, the aircraft can fly a normal soaring speed to fly, provided that variations in solar power are unrelated to whether the aircraft is climbing or cruising.

Assuming the aircraft performance is represented well by the second order polynomial equation 1 then:

$$\frac{\partial w_s(V_{cruise})}{\partial V_{cruise}} = 2aV_{cruise} + b \tag{9}$$

And equation 8 can be rewritten as:

$$\begin{aligned}0 =& w_{climb} - aV_{cruise}^2 - bV_{cruise} - c + 2aV_{cruise}^2 + bV_{cruise} \\ =& av_{cruise}^2 - c + w_{climb}\end{aligned} \tag{10}$$

Choosing the positive branch of the solution to this equation as negative airspeed is nonsensical:

$$V = \sqrt{\frac{c - w_{climb}}{a}} \tag{11}$$

Which is identical to the classic speed to fly solution.[13] Given that the solar power terms dropped out in equation 7, this result is not unexpected. One way to envision the result is that the addition of solar power simply shifts the polar up and down (i.e. modification of the "c" term) without changing the shape, effectively modifying the entire atmosphere that the aircraft flies in. While equation 11 appears to include the polar's "c" term, in fact if w_{climb} were expanded, the constant term from $w_s(V_{climb}) = aV_{climb}^2 + bV_{climb} + c$ causes the "c" to drop out of the speed to fly just as solar power did.

Some care is required in application of this theory. Nonsensical solutions exist that violate the definition of the problem. If the solar power generated is greater than the power required for level flight at the optimal speed, the time spent in cruise can be negative, clearly an unphysical result. This result simply means that if speeds greater or equal to the speed to fly can be achieved under solar power alone, it is preferable to abandon soaring and fly purely under solar power.

II.C. Solar Flight Strategies

A solar aircraft can operate without storage, with the motor consuming all of the power available from the panels. Alternatively, solar energy can be stored in an on-board battery and the motor used on command. Practical trade offs for these two approaches will be discussed further in section III.B, but first we will establish that the two approaches are energetically identical with perfect systems.

Using the same two-segment flight plan, with a constant speed descent followed by a climb in a thermal. We introduce an energy consumption factor, α. This represents the balance between using solar energy as it is produced and storing it for later use, $\alpha = 0$ indicates immediate consumption of all energy while $\alpha = 1$ corresponds to storage of all solar energy for later use.

The descent rate during the cruise segment can be written:

$$w'_{cruise} = w_s(V_{cruise}) + (1 - \alpha)p_{pv} \tag{12}$$

while the climb rate is expressed:

$$w'_{climb} = w_{climb} + p_{pv} + \alpha p_{pv} \frac{t_{cruise}}{t_{climb}} \tag{13}$$

where $t_{cruise} = \frac{h}{w'_{cruise}}$ and $t_{climb} = \frac{h}{w'_{climb}}$. Substituting and simplifying:

$$w'_{climb} = \frac{(w_{climb} + p_{pv})(w_s(V_{cruise}) + p_{pv} - \alpha p_{pv})}{w_s(V_{cruise}) + p_{pv}} \tag{14}$$

The expression for mean cross-country speed, equation 6 can then be computed. In the simplification, all terms involving the cruise-climb balance, α cancel out, so the mean cross-country speed is unaffected by the choice of when to expend energy. The time gained by extending a cruise segment is the same as that gained by shortening a climb segment. Neglecting inefficiencies in the storage system or drag caused by running the motor, the pilot has freedom to choose when to expend solar energy, provided the aircraft is equipped with a storage system.

This analysis neglects several sources of inefficiency. If the propeller is located on the nose of the aircraft, turbulence behind the propeller will increase drag on the fuselage and inboard wing.[16] In the stored energy case, there will be losses associated with charging and discharging batteries. These two effects can be analyzed in a simple way by equating the power lost to each.

$$\begin{aligned} p_{\Delta drag} &= p_{battery\ cycle} \\ \Delta C_D \frac{1}{2}\rho V^2 S_{ref} V \frac{1}{mg} &= \frac{I S_{ref} \beta \eta_{pv}}{mg} (1.0 - \eta_{cycle}) \end{aligned} \tag{15}$$

Where $\beta = \frac{S_{panel}}{S_{ref}}$ represents the fraction of the wing covered in solar cells, η_{pv} the efficiency of the conversion between sunlight and aerodynamic power, and η_{cycle} the efficiency of charging then discharging the battery. Equation 15 can be rearranged to determine the equivalent drag increment that is tolerable for a given cycle efficiency.

$$\eta_{cycle} = 1.0 - \Delta C_D \left(\frac{1}{2}\rho V^3\right)\left(\frac{1}{I\beta\eta_{pv}}\right) \tag{16}$$

Where the two grouped terms represent the dimensionalization of drag coefficient into aerodynamic power per unit wing area and specific solar power per unit wing area, respectively.

II.D. Thermal Strength Variation with Range

Thermal strength varies randomly from updraft to updraft, obviously the stronger the thermals exploited, the higher the average cross-country speed. The further an aircraft goes in between thermalling the more thermals can be evaluated (as thermals are spatially distributed), so the aircraft can more reliably exploit thermals on the tail of the distribution of thermal strengths. Thus, as sailplane performance increases the apparent thermal strength does as well, further enhancing performance.

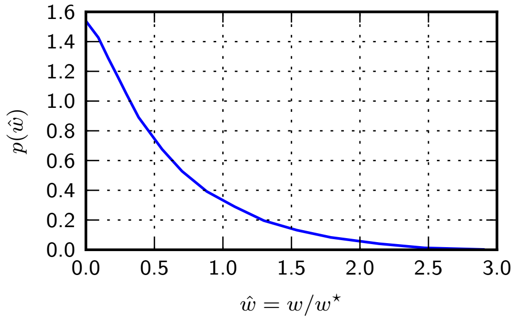

Figure 2: Probability density function for thermal strength determined by Greenhut and Khalsa.[17] Updraft strength is normalized by the convective velocity scale $w_{\star}$

Figure 2 illustrates the thermal strength probability density determined by Greenhut and Khalsa.[17] This can be used to determine how much stronger thermals appear to be as an aircraft's range increases.

A threshold is selected, representing the acceptable probability of reaching a thermal of strength $\tilde{w}$. The number of thermals that must be encountered before having confidence in encountering a thermal with the desired strength can be determined.

$$N_{required}(\tilde{w}) = \frac{\log\left(1.0 - P_{threshold}\right)}{\log \int_0^{\tilde{w}/w_{\star}} p(w/w_{\star}) d(w/w_{\star})} \tag{17}$$

Where the convective velocity scale, $w_{\star}$, can be determined from forecast models. Greenhut and Khalsa give the frequency of encountering updrafts as twice per boundary layer depth.[17] By iterating over the residual between the range of the aircraft and the range required to encounter a thermal of strength $w = \hat{w}w_{\star}$ with the desired probability, the expected thermal strength can be computed.

$$w = w_{\star}\left(\arg\min_{\tilde{w}} \left| N_{perz_i} f \frac{L}{D} - N_{required}(P_{threshold}, \tilde{w})\right|\right) \tag{18}$$

Where f gives the fraction of the boundary layer depth the aircraft traverses in a cycle, $N_{perz_i} = 2$ gives the number of thermals encountered per boundary layer depth, and $\frac{L}{D}$ gives the aircraft lift to drag ratio when flying at the inter-thermal cruise speed. Since $p(w/w_{\star})$ is a probability density function, $N_{required}$ is monotonic in the range $[0, \infty]$ so that the minimization will return the root of the absolute-valued term. While the number of thermals must be an integer, for reasonable values of $\frac{L}{D}$, f, and $P_{threshold}$ the number of thermals encountered is large so the difference between the integer and floating-point solution is small.

II.E. Solar Hybrid System

For this analysis, we assume that the solar cells are affixed to the wing only, as most other surfaces on a sailplane are relatively small. A solar to aerodynamic power efficiency of 19.4% is used after Edwards' analysis.[18] Due to connection and mass-balance issues the control surfaces are assumed to be free of cells, with 90% of the remaining wing area covered. With these constraints, panel coverage is computed based on the Discus 2 sailplane, yielding 78% of the wing area. This value is used for all three aircraft.

As sustained flight using solar power alone is not an objective, the weight of the solar power system is not addressed here. For competition sailplanes which frequently carry water ballast this is a reasonable approximation: the wing loading increase that can be obtained by water ballast is greater than the entire aircraft wing loading for most solar aircraft, and the presence of a solar augmentation system ameliorates some of the climb rate reduction from increasing weight.

For all computations a normal sun angle is assumed as the difference between normal and oblique sun angles has the same effect as varying insolation, so it is captured in the insolation analysis. The aircraft are assumed to be equipped with controllable pitch propellers so that propulsive efficiency is independent of speed. Unless otherwise noted, charging and discharging the battery is assumed to be perfectly efficient.

III. Design Space for Hybrid Soaring Vehicles

The derivations from section II provide analytic tools to understand the performance potential of low altitude hybrid soaring vehicles. The development from section II.B can be used to size the aircraft and determine achievable cross-country speed, section II.C can be used to understand the equipment and design required for the propulsion system, and section II.D to understand some of the second-order effects of a solar/soaring system on performance.

To examine the effect of aerodynamic performance, three different aircraft will be considered, covering several design points for soaring aircraft. First, the SB-XC glider used for several autonomous soaring investigations.[19,20] The Bielsko PW-5 will also be examined as an example of a modern low-performance sailplane, the Schempp-Hirth Discus 2 represents a high performance standard class sailplane.

Polars for the piloted sailplanes were generated by fitting data to the Johnson flight test reports.[21,22] The fits are weighted to ensure that the minimum sink speed and high speed performance are well represented to capture climb and cruise conditions which are more important to cross-country performance than the mid-speed range. Drag (C_L vs C_D) polars are fit that approximated the speed polars. This allows climb performance to be evaluated by directly computing the drag coefficient at climb C_L, as well as allowing changes in aircraft drag to be evaluated. The AutoSOAR speed polar is determined by applying the same process to flight test data gathered by the authors.

A thermal updraft velocity of 3 m/s is assumed for all cases, representing moderate to strong soaring conditions. Except for the solar insolation studies, the solar input is assumed to be 1000 W/m^2.

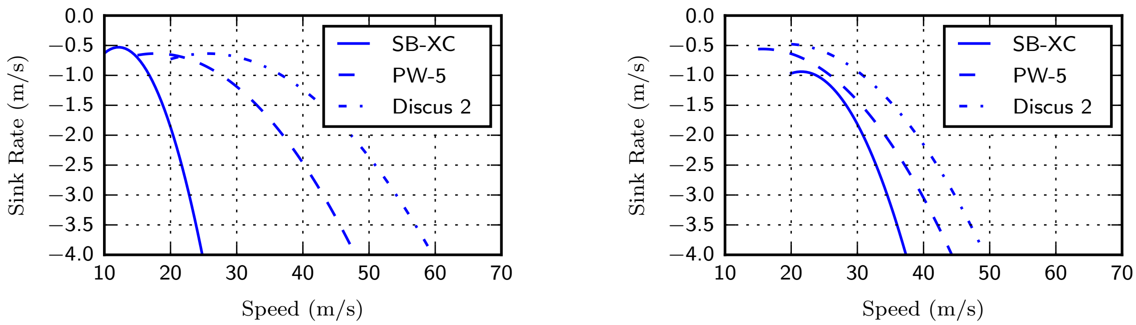

(a) The SB-XC is shown at 6.37 kg/m^2, the PW-5 at 25.8 kg/m^2, and the Discus 2 at 35.6 kg/m^2.

(b) Polars for the aircraft normalized to 30.0 kg/m^2.

Figure 3: Polars for the aircraft. Figure 3a show the polars for the aircraft at a normal wing loading. Figure 3b show the polars normalized to a common wing loading for comparison of their aerodynamic performance. In both cases, the advantage the piloted sailplanes have in high speed performance is apparent.

Figure 3 shows polars for the aircraft. At a normal operating wing loading the SB-XC exhibits a low minimum sink rate but its high speed performance falls off rapidly. When normalized to a common wing loading it is clear that the SB-XC has overall reduced performance, characteristic of model sailplanes which operate at very low Reynolds number.

III.A. Wing Loading and Aerodynamic Performance

Figure 4 illustrates the speed achievable by the Discus 2 at a range of wing loadings using different energy sources. The crossover point between soaring and solar/soaring occurs at the point where the optimal inter-thermal cruise speed crosses the speed achieved under solar power alone. This is reasonable – at that speed the aircraft has effectively an infinite $\frac{L}{D}$ at the optimal cruise speed, meaning that it thermals once and cruises forever. With increasing wing loading the cruise speed increases and thermalling becomes progressively more frequent (though initially still very infrequent as the effective $\frac{L}{D}$ is still very large).

The baseline polar of the Discus 2 is flat enough that its average speed continues to increase with wing loading, particularly evident in pure soaring flight. The gain is markedly less in hybrid flight however. As

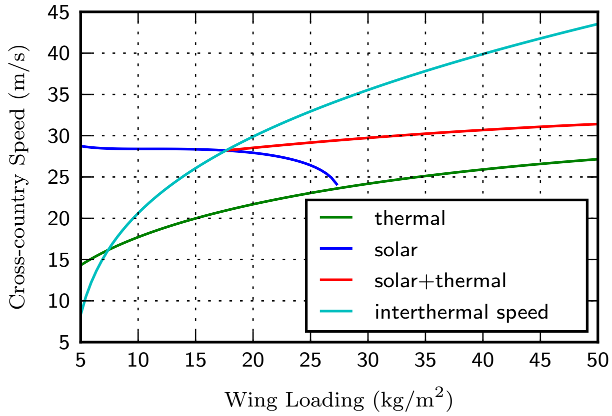

Figure 4: Speed map for the Discus 2. Hybrid soaring is more efficient once the inter-thermal cruise speed is higher than the speed achievable using solar power alone. Use of solar and soaring together improves performance and decreases the impact that wing loading has on average speed.

the mass of the aircraft increases, the specific energy provided by the solar system is reduced, counteracting the improvement in high speed performance provided by increasing the wing loading.

Figure 5 illustrates the optimal speed across a range of wing loading for each aircraft. Cases requiring a total mass below the empty weight of the aircraft are depicted in light gray. While polars can be modified to reflect differing wing loadings, the very low wing loading cases are not physically possible for the piloted sailplanes. A wing loading of 5 kg/m^2 implies a total weight approximately 1/4 of the empty weight of the PW-5.

Even if the low wing loadings cannot be achieved for the piloted sailplanes, the shape of their speed map is instructive. Since the total solar power output is a function of geometry alone, the specific power output $p_{pv} = \frac{P_{pv}}{mg}$ increases as mass decreases. In contrast, the aerodynamic performance at high speed decreases with decreasing weight as the aircraft moves to a lower, less optimal lift coefficient. If the baseline polar is flat enough that the increase in sink rate (specific power required) at high speed is less than the improvement in specific solar power, the aircraft speed can continue to increase as mass decreases. The much poorer high speed performance of the SB-XC means that the polar rather than weight drives solar-powered performance, so the polar shifting effect of greater weight is favored and maximum speed is achieved at a moderate loading.

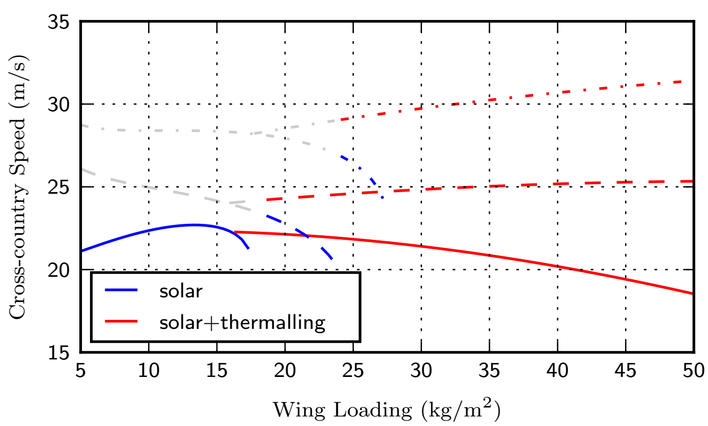

Figure 5: Comparison of cross country speeds achieved by the three aircraft. The SB-XC is in solid lines, the PW-5 in dashed, and the Discus 2 in dash-dot. Wing loadings which require a total mass below the empty weight of each aircraft are depicted in Gray.

Figure 6 illustrates the average speed that can be achieved in pure vs hybrid soaring flight over a range of wing loadings. At low wing loading the hybrid system provides enough energy to make up for the difference in aerodynamic performance between aircraft – the hybrid SB-XC outperforms the pure sailplane PW-5, and the hybrid PW-5 outperforms the pure Discus 2. The hybrid system affects average speed more than wing loading and reduces the performance gain from increasing the wing loading. In fact the hybrid PW-5 achieves nearly constant speed for a wide range of wing loading. This is because as the weight increases the specific energy provided by the solar panels decreases, reducing the benefit of hybridization.

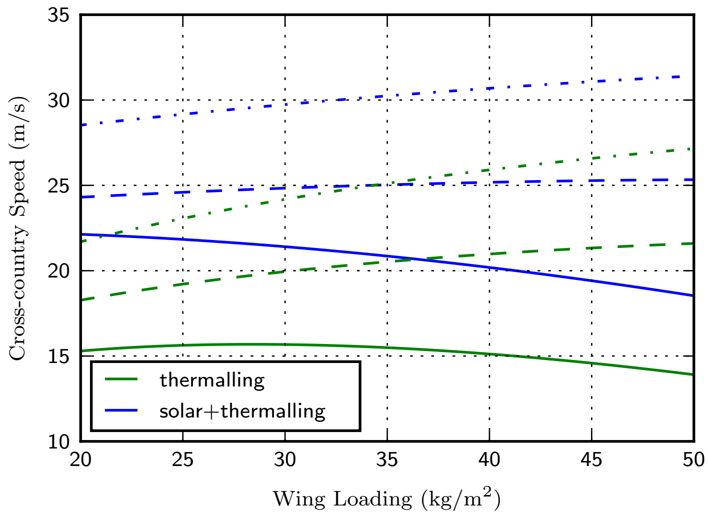

Figure 6: Comparison of soaring cross country speeds achieved by the three aircraft, lines as in figure 5. Hybrid soaring makes more of an impact than wing loading on average speed and in some circumstances can make up for differences in aerodynamic performance between classes of aircraft.

III.B. Energy Storage

Section II.C discussed analysis of two strategies for motor usage. Approximating the propeller effect as inducing turbulent flow on the fuselage, the drag coefficient is increased by two counts.[23] Equation 16 can be used to compute the equivalent battery cycle efficiency. A more in-depth analysis is also performed. Increased drag is simulated by adding two counts to the drag polars and then computing modified speed polars. Battery round-trip losses are evaluated by multiplying η_{pv} by η_{cycle}, in both cases performance can be analyzed as in section III.A. Table 1 summarizes the equivalent efficiency, as well as the performance loss for increased drag and for an 80% efficient cycle.

	SB-XC	PW-5	Discus 2
η_{cycle} equivalent to $\Delta C_D = 0.002$ (%)	78.7	69.7	53.7
$\Delta V_{mean}, \Delta C_D = 0.002$ (m/s)	-1.39	-1.33	-2.34
$\Delta V_{mean}, \eta_{cycle} = 0.8$ (m/s)	-1.07	-1.0	-1.2

Table 1: Performance impact from battery charge/discharge cycle efficiency and drag increment due to running propeller. Computations are performed for a thermal updraft strength of 3.0 m/s, solar insolation of 1000 W/m^2, sea level density, and wing loading of 30.0 kg/m^2.

The equivalent cycle efficiency follows the trend expected – the higher performance sailplanes fly faster in cruise and are less tolerant of drag increases, in the case of the Discus 2 a cycle efficiency near 50% is preferable to the drag increase. Trends in the impact on speed are less clear, with the speed decrease for the

PW-5 falling intermediate to the other two aircraft, it is clear however that across classes of sailplanes, drag reduction is more critical than improving propulsive efficiency.

Table 1 also illustrates that the simple analysis from equation 16 understates the impact that drag can have: the SB-XC equivalent efficiency is near that analyzed using the more advanced analysis, but increasing drag impacts average speed more than reducing the cycle efficiency. This is because the drag increase also influences the speed to fly. Degrading aerodynamic performance causes the optimal speed to fly to decrease in addition to slowing climb rate whereas reduced propulsive efficiency only impacts climb rate.

While the previous analysis indicates that energy storage offers a performance advantage, it is important to verify that storage requirements are reasonable. The energy which must be stored scales with the time between motor runs. Assuming that the motor is used during every climb, then this can be expressed in terms of the inter-thermal sink rate and depth of the layer worked.

Frequent use of the motor requires relatively modest storage – the specific energy stored in the battery is less than the working layer depth (if it was greater then continuous solar flight would be possible). The specific energy that must be stored for different layer depths is depicted in figure 7a.

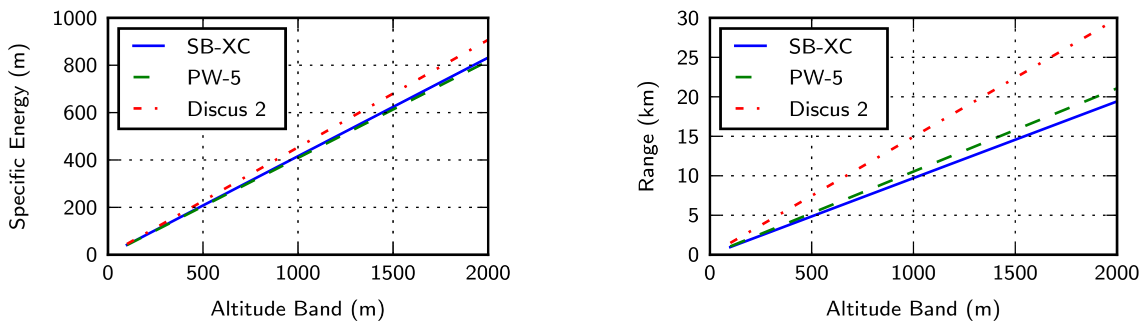

(a) Specific energy that must be stored for the three aircraft as a function of the thermal climb depth assuming that the energy gained in a cruise segment is expended to assist the next climb.

(b) Range provided by the energy stored at the end of a cruise segment if the aircraft continues to cruise at the inter-thermal speed.

Figure 7: Energy storage required and range that can be achieved with that energy for each aircraft. Thermal strength is 3 m/s, and all aircraft are loaded at 30 kg/m^2.

The amount of energy is similar for each aircraft – for given atmospheric conditions optimal glider descent rates are similar, performance differences between aircraft are due more to the speed at which a given sink rate occurs. This is illustrated by the range each aircraft achieves for the stored energy, illustrated in figure 7b. The mass required to store the solar energy is quite reasonable, even with a 2000 meter working depth less than 2% of the aircraft mass must be storage assuming battery specific energy comparable to the FES system.[24] From an operational perspective, an aircraft could be equipped with modular battery packs allowing the pilot to select the amount of storage desired before flight similar to selecting the mass of water ballast to carry in conventional sailplanes.

III.C. Range Increase

The analysis of performance improvement from the energy perspective does not capture the disproportionate benefit that extending cruise range can have. As cruise range increases, the aircraft is more likely to reach a stronger thermal. Under the conditions analyzed, continuous use of solar power extends the range of the PW-5 by approximately 70%, substantially increasing the likelihood of reaching a strong thermal.

When storing solar power and using it in climb, the PW-5 has a range of 26 km assuming the updraft strength is 3.0 m/s and the aircraft climbs 1 km. Continuous use of solar power extends this to 44 km. Note that the increment in range is greater than would be computed by adding 26 km to the value from figure 7b because as the aircraft flies the additional distance it continues to harvest solar energy, further increasing range.

Equation 18 can be used to estimate the enhancement in updraft strength due to this increase in range.

Specifying a 95% chance of finding a thermal of a given strength as a benchmark, a baseline updraft of 3.0 m/s (the strength encountered with a range of 26 km), and assuming the aircraft works half of the boundary layer depth, the range increase from continuously running the motor allows the aircraft to reach a thermal 15% stronger. This translates into a increase in mean speed of approximately 5% or 1.3 m/s. This difference would mean 4-5 places on many days during world championships and is approximately equal to the penalty from running the motor.

Combined with the results of section III.B, this suggest blending the storage and range extending strategies: flying as a pure sailplane, then running the motor if a strong thermal is not encountered before reaching the bottom of the desired altitude band.

III.D. Impact of Solar Input

Solar input will vary with season, time of day, location, and weather conditions. This introduces a design challenge similar to anticipating thermal strength. While figure 6 showed that hybrid solar/soaring aircraft are less sensitive to wing loading than pure sailplanes, sensitivity is dependent on solar input. Figure 8 illustrates the relationship between insolation, wing loading, and speed. Speed is linearly related to insolation, but as the solar energy available decreases, the sensitivity to wing loading increases.

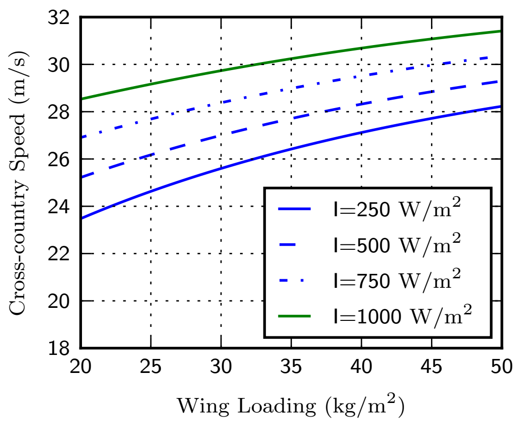

Figure 8: Mean cross-country speed for the Discus 2 at several solar insolation values. The speed variation with wing loading is greater as insolation decreases and the aircraft is more dependent on thermals. Thermal strength is 3 m/s.

The improvement in the high speed polar caused by increasing the wing loading is offset by the reduction in specific energy input from the solar cells. This effect can be substantial, evidenced by the nearly flat speed achieved by the PW-5 in figure 6. As insolation decreases, solar energy is less able to compensate for changes in the polar so the cross-country speed is more a function of the sailplane's aerodynamic performance.

The linear relationship between insolation and speed can be traced back to equation 6. As the solar input does not appear in the optimization for speed to fly, the only impact that solar input has on average cross-country speed is the balance of time spent thermalling vs cruising.

IV. Conclusions

Using soaring speed to fly theory, optimal speed to fly is demonstrated to be independent of solar power harvested. Average cross-country speed is shown to be independent of when the energy is utilized for a perfect storage and propulsion system, and a method is established to equate different types of propulsion-related inefficiencies. Finally, the statistical distribution of thermal strengths is used to develop an expression for the effect of aircraft range on the strength of thermal available.

These developments are used to analyze the performance of solar/soaring hybrid aircraft. The effect of aerodynamic efficiency is explored by examining several existing sailplane designs. For each design, performance sensitivity to wing loading, solar insolation, and solar exploitation strategy is explored to identify key features for hybrid sailplanes.

In many respects hybrid solar/soaring aircraft design is very similar to design of conventional sailplanes. For high performance designs, increasing wing loading improves average speed, though performance is less sensitive to loading for hybrids than conventional sailplanes. For very efficient designs, hybrid aircraft can achieve higher speeds than pure solar aircraft at the expense of not being able to fly on solar power alone. For applications beyond racing sailplanes, lower performance designs can sustain high speeds while carrying payloads that would not be feasible flying purely under solar power.

Achieving low drag is as critical for hybrid as for pure soaring aircraft. When sized for racing, a solar augmented aircraft can tolerate substantial propulsive inefficiency in the pursuit of low cruise drag. This suggests that designers should devote considerable effort to positioning propellers in locations that minimize the added drag when the motor is running. Even beyond racing aircraft, high-speed performance is important as a purely solar powered aircraft will operate well into the high speed region of its polar when cruising.

Solar augmentation raises questions for what it means for an aircraft to be a sailplane, and adds complexity to design, manufacture, and piloting. The performance advantage is considerable however, in many cases making up for the difference in performance between classes of aircraft. Augmentation with solar power has the potential to enhance sailplane performance by a degree similar to the introduction of composite construction while retaining the philosophy of utilizing only the energy available in the environment. In this light it is worth considering as an avenue for future sailplane design.

References

[1]Boucher, R. J., "History of solar flight," *20th Joint Propulsion Conference*, 1984.

[2]Noth, A., "History of Solar Flight," Tech. rep., ETH Zurich, 2008.

[3]Oettershagen, P., Melzer, A., Mantel, T., Rudin, K., Lotz, R., Siebenmann, D., Leutenegger, S., Alexis, K., and Siegwart, R., "A Solar-Powered Hand-Launchable UAV for Low-Altitude Multi-Day Continuous Flight," *IEEE International Conference on Robotics and Automation*, 2015, pp. 3986–3993.

[4]Christopher, R., *Extending the endurance of small unmanned aerial vehicles using advanced flexible solar cells NAVAL POSTGRADUATE*, Master's, Naval Postgraduate School, 2012.

[5]Cocconi, A., "AC Propulsion's Solar Electric Powered Solong UAV," Tech. rep., AC Propulsion, 2004.

[6]Rehmet, M. and Kroplin, B.-H., "Human Flight with Light," *Technical Soaring*, Vol. 21, No. 2, 1996, pp. 36–43.

[7]Travierso, M., "Five Electric Planes to Watch," *IEEE Spectrum*, aug 2013, pp. 9–11.

[8]Duranti, P., "Electrical- and Sun- Powered Gliders: Do They Require a Definition of New F.A.I Classes," *Technical Soaring*, Vol. 22, No. 3, 1998, pp. 66–73.

[9]Hirth, W., *The Art of Soaring Flight*, 1938.

[10]Barnaby, R. S., *Gliders and Gliding*, Ronald Press Company, 1930.

[11]MacCready, P. B. J., "Optimum Airspeed Selector," *Soaring*, , No. 1, 1958, pp. 10–11.

[12]Arho, R., "Optimal Dolphin Soaring as a Variation Problem," *Technical Soaring*, Vol. III, No. 1, 1973, pp. 20–26.

[13]Reichmann, H., *Cross-Country Soaring*, Soaring Society of America, 1981.

[14]Stojkovic, B., "Generalized Speed-to-Fly Theory," *Proceedings of the XXII OSTIV Congress*, Uvalde, Texas, USA, 1991, pp. 77–83.

[15]Almgren, R. and Tourin, A., "Optimal Soaring via Hamilton-Jacobi-Bellman Equations," *SSRN Electronic Journal*, 2014, pp. 1–24.

[16]Miley, S. J., Howard, R. M., and Holmes, B. J., "Wing laminar boundary layer in the presence of a propeller slipstream," *Journal of Aircraft*, Vol. 25, No. 7, 1986, pp. 606–611.

[17]Greenhut, G. K. and Khalsa, S. J. S., "Updraft and downdraft events in the atmospheric boundary layer over the equatorial pacific ocean," 1982.

[18]Edwards, D. J., Kahn, A. D., Kelly, M., Heinzen, S., Scheiman, D. A., Jenkins, P. P., Walters, R., and Hoheisel, R., "Maximizing Net Power in Circular Turns for Solar and Autonomous Soaring Aircraft," *Journal of Aircraft*, jan 2016, pp. 1–11.

[19]Edwards, D. J. and Silverberg, L. M., "Autonomous Soaring: The Montague Cross-Country Challenge," *Journal of Aircraft*, Vol. 47, No. 5, 2010, pp. 1763–1769.

[20]Allen, M. J., "Guidance and control for an autonomous soaring UAV," Tech. rep., NASA Dryden Flight Research Center, 2007.

[21]Johnson, R. H., "A Flight Test Evaluation of the Discus 2B Standard Class Racer," *Soaring1*, may 1999, pp. 32–36.

[22]Johnson, R. H., "A Flight Test Evaluation of the PW-5 World Class Sailplane," *Soaring*, apr 1997, pp. 19–23.

[23]Boermans, L. M. M., "Wind Tunnel Tests of Eight Sailplane Wing-Fuselage Combinations," *Technical Soaring*, Vol. 8, No. 3, 1983, pp. 70–85.

[24]King, J., "FES is Changing Soaring as We Know it," *Gliding International*, 2016, pp. 46–49.